*Progress In Electromagnetics Research C, Vol. 26, 229–243, 2012*

# MINIATURIZED DUAL-MODE RESONATORS WITH MINKOWSKI-ISLAND-BASED FRACTAL PATCH FOR WLAN DUAL-BAND SYSTEMS

**J. C. Liu[1,*], H. H. Liu[1], K. D. Yeh[1], C. Y. Liu[2], B. H. Zeng[3], and C. C. Chen[4]**

[1]Department of Electrical Engineering, Ching Yun University, Chung-Li, Tao-Yuan 32097, Taiwan, R.O.C.

[2]Department of Electronic Engineering, Tahwa Institute of Technology, Qionglin, Hsinchu 307, Taiwan, R.O.C.

[3]Department of Antenna Business Division, LOROM Group, Taipei, Taiwan, R.O.C.

[4]Department of Electrical Engineering, Feng-Chia University, Taichung 40724, Taiwan, R.O.C.

**Abstract**—The miniaturized dual-mode dual-band band-pass filters (BPF) using Minkowski-island-based (MIB) fractal patch resonators are proposed in this paper. The BPF is mainly formed by a square patch resonator in which a MIB fractal configuration with 2nd order iteration is embedded in the patch. By perturbation and inter-digital coupling, the wide-band and dual-band responses are obtained respectively. For miniaturized wide-band design, at 2.41 GHz central frequency it has good measured characteristics including the wide bandwidth of 2.26–2.56 GHz (3-dB fractional bandwidth of 12.4%), low insertion loss of 0.72 dB, high rejection level (−52.5/−44.9 dB), and a patch size reduction with 60.6%. For compact dual-band design, the proposed filter covers the required bandwidths for WLAN bands (2.20–2.96 GHz and 4.74–5.85 GHz). The patch size reduction of 78.1% is obtained. Two transmission zeros are placed between the two pass-bands and resulted in good isolation.

*Received 15 November 2011, Accepted 28 December 2011, Scheduled 5 January 2012*

* Corresponding author: Ji Chyun Liu (jichyun@cyu.edu.tw).

## 1. INTRODUCTION

The dual-mode, introduced by Wolff [1], could be implemented on a microstrip resonator. This characteristic was usually applied to realize band-pass filters in microstrip circuits. Dual-mode filters have been widely used in wireless communications systems because of their advantages in applications such as small size and low loss. As is well known, there are several commonly used dual-mode patch resonators including crossed slots [2, 5], loaded crossed-slots [3], right crossed-slots [4, 7, 10, 14], SIR [6], slot etched [15], and fractal configurations [8, 9, 11–13, 16] in a square patch. For miniaturization, five patches centered at 1.53, 1.595, 2.40, 14.125, and 2.15 GHz, with the size reductions of 50% [3], 58% [4], 24% [10], 53% [13], and 74% [15] respectively were proposed.

The patch resonator with a pair of tilted crossed slots was first proposed for the filter design having the size and loss reduction simultaneously [2], and the patch resonators using inductively loaded crossed-slots or right crossed-slots are used to reduce the loss and to generate the BPF with transmission zeroes. Recently, the dual-mode filters with Sierpinski-based fractal resonator were introduced [8, 9, 11]. The alternative fractal-shaped BPF was applied for UWB applications [12], and the MIB fractal patch resonators were applied [13, 16]. The iterative configurations consisted in etching each side of the square patch with a space-to-side ratio = 1/7. It was a lower ratio fractal patch resonator [13]. Meantime, the dual-mode fractal patch resonator with miniaturization was applied to achieve a wide-band system [16]. The basic characteristics of the fractal geometry are space-filling and self-similarity. Space-filling technique is applied to miniaturization and self-similarity is used to obtain wide-band and multi-band responses. Thus, the fractal patch resonator for dual-mode BPF design is an interesting topic to study.

The increasing demand for multi-band applications has required a single wireless transceiver to support multi-band operations. The dual-band BPF plays an important role in a multi-band transceiver [17–25]. Applied to 2.4 and 5.2 GHz dual-band systems, a coupled-serial-shunted line structure was designed [17]. The parallel-coupled and vertical-stacked SIR configurations were used at 2.45/5.2 GHz or 2.45/5.8 GHz dual-band [18]. The compact ring dual-mode resonator with 2.4/5.2 GHz dual-band was proposed [19]. The dual-mode ring resonator with periodically-loaded open stubs was presented with 2.4/5.8 GHz dual-band [23]. However, WLAN systems combining 2.4, 5.2, and 5.8 GHz are becoming more attractive. Especially for universal applications, it should be covering the whole 2.4–2.5 GHz and 5.15–

5.85 GHz bands for the WLAN systems. Thus, a dual-band and wideband filter is a key component for such WLAN systems.

In this article, we propose a novel dual-mode BPF by using a 2nd order MIB fractal resonator. The fractal patch resonator with a space-to-side ratio = 1/3 is constructed. It was a higher ratio fractal patch resonator and much space can be obtained. Minkowski-island is a plane fractal configuration described in 1997. Cohen proposed the antenna with miniaturization and multi-band responses based on Minkowski-island fractal [26]. First, by increasing the iteration order of MIB fractal resonator, the resonant frequency can be moved towards the lower frequency, indicating a miniaturized property. Second, adding a perturbation element at the corner of the MIB fractal resonator, the various dual modes can be found in a wide-band response. Consequently, a 2nd order MIB fractal resonator is used to design a high performance dual-band BPF at WLAN 802.11a/b/g systems. Finally, the dual mode BPF is implemented and then measured, and the simulation responses are well confirmed by the measured results.

## 2. CONFIGURATIONS AND BASIS

### 2.1. Dual-mode Square Patch Resonators with Perturbation

For dual-mode square patch, the typical resonator, crossed slots, right crossed-slots, slot etched, MIB fractal resonator, and Sierpinski-based fractal resonator are used for designing the BPF and shown in Figures 1(a) to (f), respectively. Both input and output ports are spatially separated 90° from each other, and put perturbations such as a patch in corner are located 135° offset from input and output ports and the basic dual-mode square-loop resonator BPF is established.

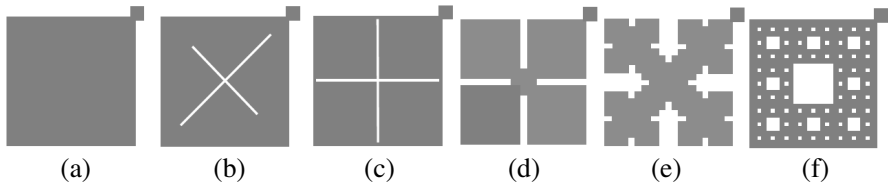


**Figure 1.** Dual-mode square patch resonators. (a) Typical resonator. (b) Crossed slots. (c) Right crossed-slots. (d) Slot etched. (e) MIB fractal resonator. (f) Sierpinski-based fractal resonator.

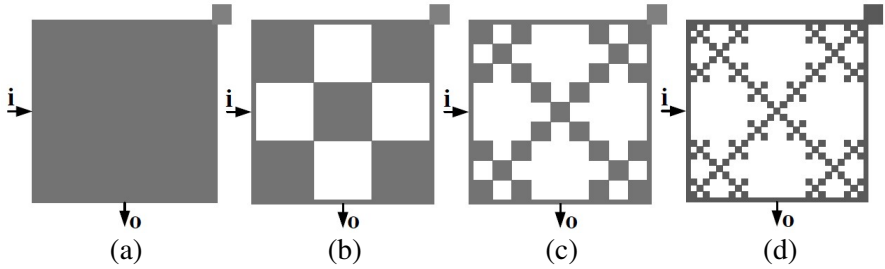


**Figure 2.** Iterative configurations of Minkowski-island fractal. (a) Original. (b) 1st order. (c) 2nd order. (d) 3rd order.

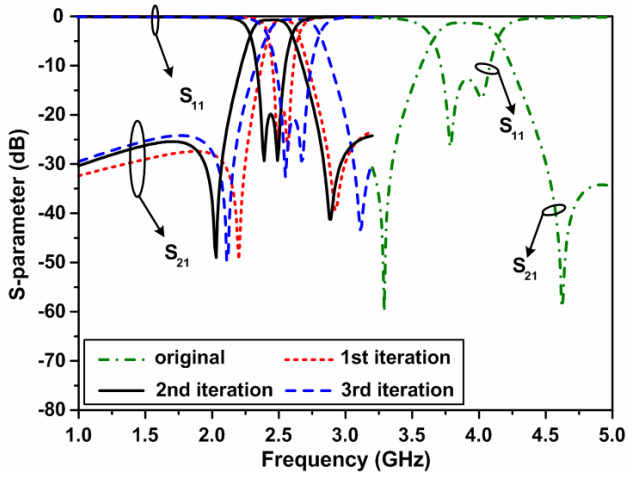


**Figure 3.** Frequency responses of iterations in MIB fractal resonator.

## 2.2. Minkowski-island Based Fractal Configurations

In Figures 2(a), (b), (c), and (d), the iterative configurations of Minkowski-island based fractal are presented. Figure 2(a) is the original patch, Figure 2(b) is the 1st order iteration patch, Figure 2(c) is the 2nd order iteration patch, and Figure 2(d) is the 3rd order iteration patch.

For comparison, all the patches are approximately equal, and the detail dimensions of the resonators are listed in Table 1. The responses are shown in Figure 3, and the simulation results are tabulated in Table 2. When the iteration order increases, the space and the island in each patch are different, and the central frequency, the bandwidth, and the transmission zeros are varied. The created space mainly influences

**Table 1.** Dimensions of the MIB fractal resonators.

| Dimensions (all in mm) | Original patch | 1st order fractal patch | 2nd order fractal patch | 3rd order fractal patch |
|---|---|---|---|---|
| $L_1$ | 11.10 | 11.10 | 11.05 | 11.05 |
| $L_2$ | 3.7 | 5.7 | 7.7 | 7.7 |
| $W_1$ | 2.3 | 2.3 | 2.3 | 2.3 |
| $W_2$ | 3.0 | 3.0 | 3.0 | 3.0 |
| $W_3$ | 0.5 | 0.5 | 0.5 | 0.5 |
| $W_4 = W_5$ | - | - | 1.15 | 1.15 |
| $W_6$ | - | 3.45 | 3.45 | 3.45 |
| $W_7$ | 0.1 | 0.15 | 0.2 | 0.2 |
| $W_8$ | - | 0.4 | 0.3 | 0.3 |
| $W_{p1} = W_{p2}$ | 1.9 | 1.9 | 1.9 | 1.9 |
| $G$ | 0.1 | 0.15 | 0.2 | 0.2 |

**Table 2.** Frequency responses of the MIB fractal resonators.

| Simulation | | Original patch | 1st order fractal patch | 2nd order fractal patch | 3rd order fractal patch |
|---|---|---|---|---|---|
| $f_0$ (GHz) | | 3.89 | 2.53 | 2.44 | 2.60 |
| $-3$ dB BW (MHz) | | 400 | 190 | 280 | 360 |
| Fractional BW (%) | | 10.30 | 7.50 | 11.47 | 13.84 |
| Min insertion loss (dB) | | $-1.34$ | $-0.95$ | $-0.73$ | $-0.60$ |
| Resonances (GHz) | Even | 3.79 | 2.49 | 2.39 | 2.55 |
| | Odd | 4.01 | 2.57 | 2.49 | 2.67 |
| Transmission zeros (dB) | Lower | $-57.1$ | $-47.8$ | $-48.7$ | $-49.5$ |
| | Upper | $-58.7$ | $-39.3$ | $-41.5$ | $-43.3$ |
| Patch size reduction | | - | 57.7% | 60.6% | 55.3% |

the central frequency which shifted down in the spectrum as the space increases. Self-similarity islands spread the bandwidth.

As the 1st order iteration patch, the space occupies about 44% area of the patch, and it has 5 islands. The central frequency of the 1st order iteration patch is dramatically lowered to 2.53 GHz as opposed to 3.89 GHz of the original patch for the fixed side length. It implies that the side length of the patch is reduced by 57.7% if the operating frequency keeps unchanged.

For the 2nd order iteration patch, the space presents about 64% area of the patch, and it has 25 islands. The central frequency

shifts from 2.53 to 2.44 GHz related to the 1st order iteration patch. Meanwhile, the fractional BW spreads from 7.50% to 11.47%. Finally, for the 3rd order iteration patch, the space required is about 66% area of the patch, only 2% more than the 2nd order iteration patch; however, it has 125 islands. Although the fractional BW extents from 11.47% to 13.84%, the central frequency rises slightly because of the high-frequency effects of the smaller islands. It is found that applying the second order of MIB fractal, the resonant frequency can be moved towards the lower frequency, indicating a miniaturized property with a patch size reduction about 60.6%. In addition, the 3rd order iteration patch has much smaller islands, and it could have the fabrication inaccuracies. Thus, the 2nd order iteration patch with identical islands is a suitable approach for accurate design.

## 3. DUAL-MODE WIDE-BAND BPF WITH 2ND ORDER MIB FRACTAL RESONATOR

Dual-mode wide-band BPF with 2nd order MIB fractal resonator is proposed in Figure 4. The dimensions of the proposed filter are $L_1 = 11.05\,\text{mm}$, $L_2 = 7.7\,\text{mm}$, $W_1 = 2.3\,\text{mm}$, $W_2 = 3.0\,\text{mm}$, $W_3 =$

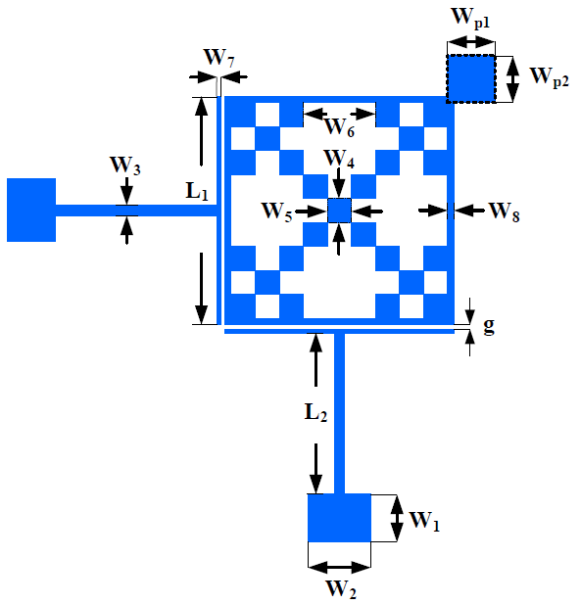


**Figure 4.** Wide-band Minkowski-island-based fractal resonator.

0.5 mm, $W_4 = 1.15$ mm, $W_5 = 1.15$ mm, $W_6 = 3.45$ mm, $W_7 = 0.2$ mm, $W_8 = 0.3$ mm, $g = 0.2$ mm and $W_{p1} = W_{p2} = 1.9$ mm.

The simulations for the proposed filter are achieved with IE3D [27]. In contrast to the FR4 substrate and the input and output directive couplings used in the previous works [16], the Duriod-6010 substrate with dielectric constant $\varepsilon_r = 10.2$, $\delta = 0.0023$, thickness $h = 1.27$ mm ($\leq 0.03\lambda g$) is used and the improved T-couple is proposed. The effective dielectric constant is $\varepsilon_{eff} = 8.11$ and guided wavelength is $\lambda g = 43.2$ mm at frequency $f_0 = 2.44$ GHz. The patch size is $11.05 \times 11.05$ mm$^2$ ($0.25\lambda g \times 0.25\lambda g$).

The proposed filter is simulated and measured in Figure 5. The dominant mode ($TM_{110}$) is considered. Both simulated and measured results are in good agreement. The dual-mode occurs within the wideband responses and two transmission zeros are observed. For measurement results, at a center frequency of 2.41 GHz, wide bandwidth of 2.26–2.56 GHz (3-dB fractional bandwidth, FBW = 12.4%), low insertion loss of 0.72 dB, and deep transmission zeros of $-52.5$ and $-44.9$ dB are presented. The stop-band extended to $2.0f_0$ is below $-23$ dB rejection level. In contrast to the original patch resonator shown in Figure 5, the patch size reduction of 60.6% is obtained in the proposed filter.

The variations of the perturbation are investigated in Figure 6. As perturbation increases, 1.8 mm $\leq W_{p1} \leq$ 2.4 mm, the dual-mode deviation increases, and the coupling coefficients ($k = (f_o^2 - f_e^2)/(f_o^2 + f_e^2)$) increase.

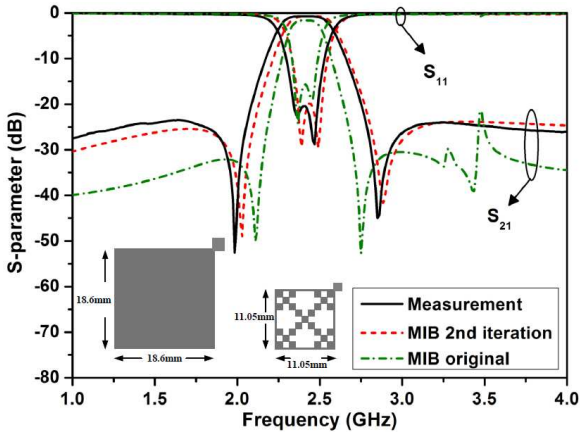


**Figure 5.** Frequency responses of 2nd order iteration MIB fractal resonator.

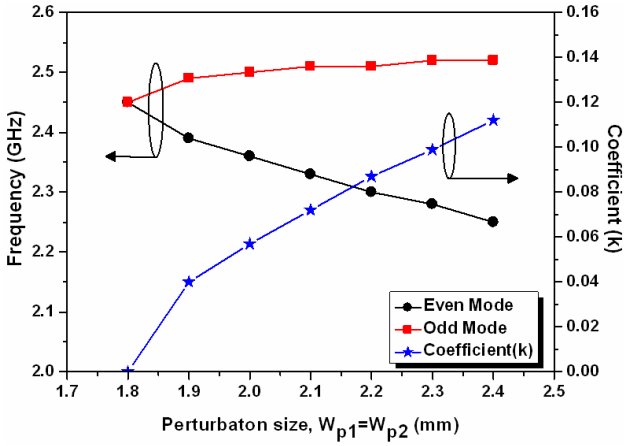


**Figure 6.** Dual-mode split characteristics.

### 3.1. Dual-mode Dual-band BPF with 2nd Order MIB Fractal Resonator

For the design of a resonator using a novel inter-digital coupling, the dual-mode dual-band BPF with 2nd order MIB fractal resonator is proposed in Figure 7. The dimensions of the proposed filter are $L_1 = 8.7\,\text{mm}$, $L_2 = 6.05\,\text{mm}$, $W_1 = 2.0\,\text{mm}$, $W_2 = 2.0\,\text{mm}$, $W_3 = 0.2\,\text{mm}$, $W_4 = 0.2\,\text{mm}$, $W_5 = 0.9\,\text{mm}$, $W_6 = 0.9\,\text{mm}$, $W_7 = 2.7\,\text{mm}$, $W_8 = 0.3\,\text{mm}$, $W_9 = 2.15\,\text{mm}$, $g_a = 0.25\,\text{mm}$, $g_b = 0.2\,\text{mm}$ and $W_{p1} = W_{p2} = 3.23\,\text{mm}$.

The proposed filter is simulated and measured in Figure 8. Both $\text{TM}_{110}$ and $\text{TM}_{210}$ modes are considered. Both simulated and measured results are in good agreement. The dual-mode occurs within the dual-band responses and two transmission zeros (4.07 GHz and 4.51 GHz) are placed between the two pass-bands and resulted in a good isolation ($-22\,\text{dB}$).

For the first pass-band, at center frequency of 2.55 GHz, wide bandwidth of 2.20–2.96 GHz (3-dB fractional bandwidth, FBW = 29.8%), low insertion loss of 0.35 dB, and deep transmission zeros of $-46.7$ and $-44.2\,\text{dB}$ at 1.93 GHz and 4.07 GHz are obtained. For the second pass-band, at center frequency of 5.27 GHz, wide bandwidth of 4.74–5.85 GHz (3-dB fractional bandwidth, FBW = 21%), low insertion loss of 0.86 dB, and deep transmission zeros of $-37.8$ and $-65\,\text{dB}$ at 4.51 GHz and 6.89 GHz are presented.

Figure 9 presents the surface current distributions of the proposed filter. In the pass-band, the square patches around the edge side

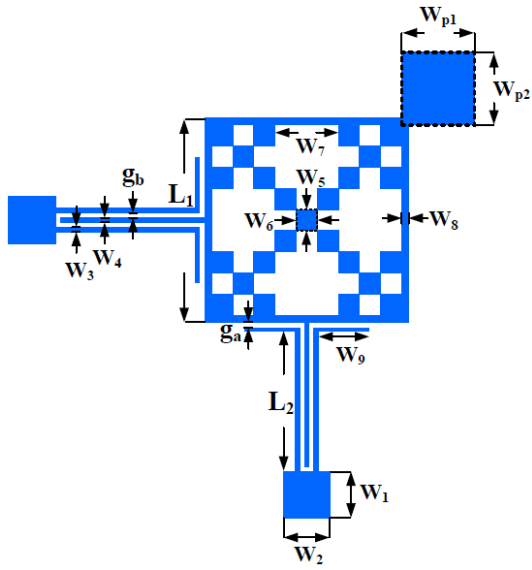


**Figure 7.** Dual-band Minkowski-island-based fractal resonator.

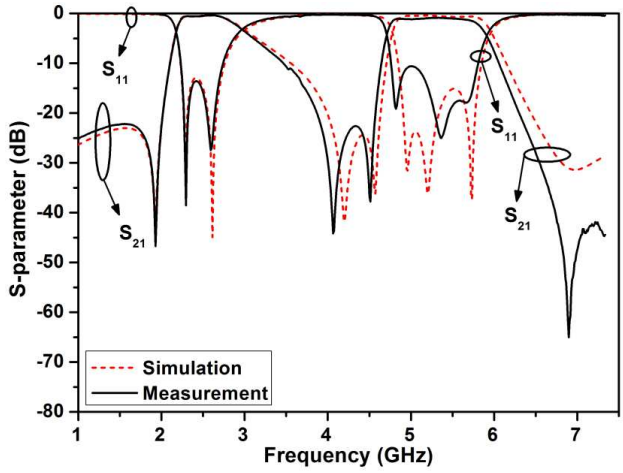


**Figure 8.** Dual-band frequency responses of 2nd order iteration MIB fractal resonator.

exhibit the identical surface current distributions with the electrical path according to the resonances. At 2.28 and 2.60 GHz resonances of the first pass-band and 4.95, 5.20 and 5.73 GHz resonances of the

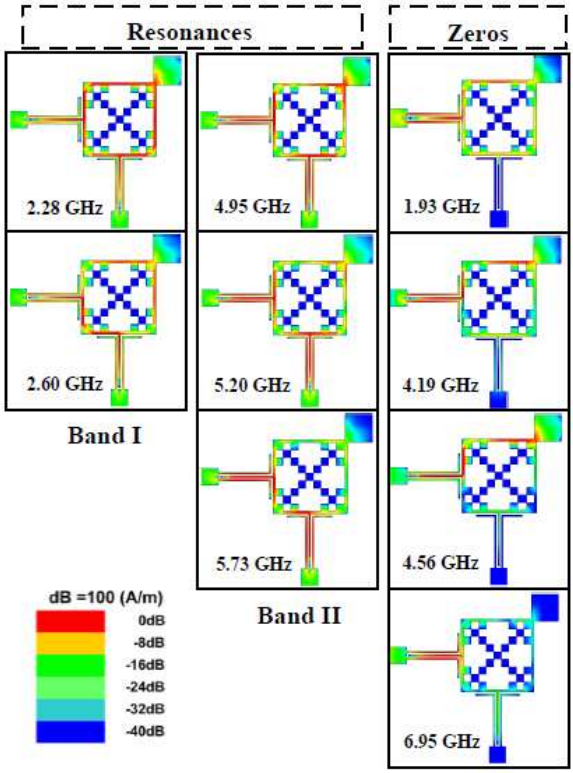


**Figure 9.** Surface current distributions.

second pass-band, the input currents flow via the input ports and couple almost completely to the output ports.

The even (2.28 GHz) resonance has current maxima at the corner (135°) of the patch. The odd (2.60 GHz) resonance has current maxima at the edge side (90°) of the patch. At 1.93, 4.19, 4.56 and 6.95 GHz resonances, which are the four transmission zeros of the filter, the input signals are completely reflected back at the input ports and no currents flow in the output ports.

The variations of the perturbation are investigated in Figure 10. As perturbation increases, $2.8\,\text{mm} \leq W_{p1} \leq 3.6\,\text{mm}$, the dual-mode dual-band deviation increases. The photographs of the filters are presented in Figure 11. The left one is the dual-band filter, and the right one is the wide-band filter. In contrast to the original patch resonator shown in Figure 5, the patch size reduction of 78.1% is obtained in the dual-band filter.

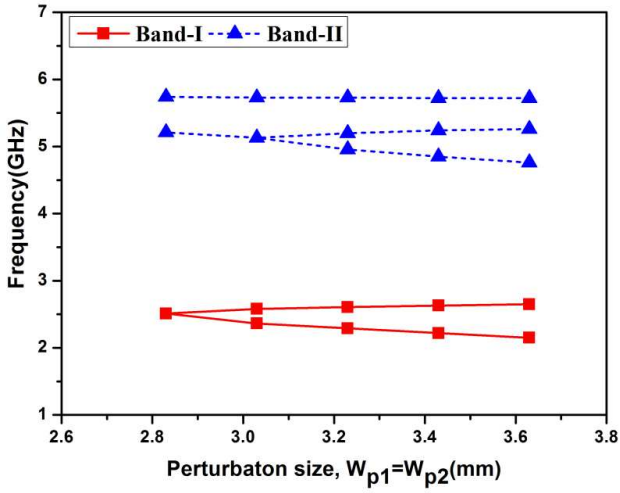


**Figure 10.** Dual-mode dual-band split characteristics.

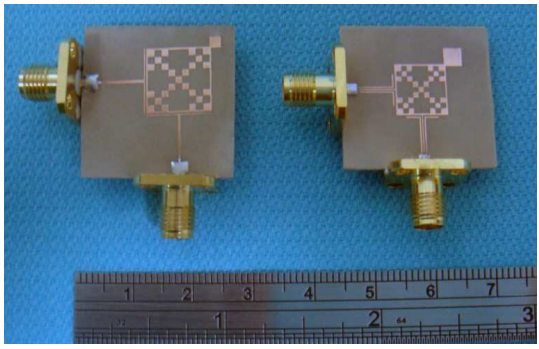

**Figure 11.** The photograph of the proposed filters.

Since the square patches around the edge side exhibit the identical surface current distributions with the electrical path according to the resonances, we can design the MIB fractal patch by using square loop resonator. For a square loop resonator, the mean circumference of the loop is equal to an integral multiple of the guided wavelength, the resonance is established as:

$$4L_1 = n\lambda_g, \quad n = 1, 2, 3, \ldots \tag{1}$$

where $L_1$ = side length of the loop, $\lambda_g$ = guided wavelength.

The guided wavelength is written as:

$$\lambda_g = \frac{\lambda_0}{\sqrt{\varepsilon_{eff}}} \tag{2}$$

where $\lambda_0$ = wavelength in free space, $\varepsilon_{eff}$ = effective dielectric constant.

The resonated frequency is expressed as:

$$f_n = \frac{nc}{4L_1\sqrt{\varepsilon_{eff}}}, \quad n = 1, 2, 3, \ldots \tag{3}$$

As $n = 1$, the central frequency $f_1$ in first band is obtained. When $n = 2$, the central frequency $f_2$ in second band is presented.

The effective design procedure is provided:

1. According to the central frequencies of the desired two bands, the circumference of the patch is equal to the guided wavelength, and the side dimension of the patch is determined by (1) to (3).
2. Increasing the perturbation size and splitting the dual-mode, the bandwidth is obtained.
3. Changing the iteration order, the central frequency, the bandwidth, and the transmission zeros are adjusted.
4. Designing a novel inter-digital coupling, the dual-mode dual-band BPF is achieved.

## 4. CONCLUSIONS

A miniaturized dual-mode MIB BPF with wide-band and dual-band responses, low insertion-loss and two transmission zeros is proposed in this paper. The space-filling technique and the self-similarity of the iterative fractal configuration is an available approach to achieve the miniaturization, the BW extension and the transmission zero adjustment. By tuning the perturbation, dual-mode resonances are excited for the desired wide-band responses.

The performance with wide bandwidth (FBW = 12.4%), low insertion loss (0.72 dB), high rejection level (−52.5/−44.9 dB), and the size reduction with 60.6% are achieved at center frequency of 2.41 GHz for wide-band applications. These filters can achieve a wide pass band and sharp rejection band. It can be applied to the WLAN 802.11b/g systems.

For the dual-band applications, at first center frequency of 2.55 GHz, wide bandwidth of 2.20–2.96 GHz (3-dB fractional bandwidth, FBW = 29.8%), low insertion loss of 0.35 dB, and deep transmission zeros of −46.7 and −44.2 dB at 1.93 GHz and 4.07 GHz are

obtained. For the second center frequency of 5.27 GHz, wide bandwidth of 4.74–5.85 GHz (3-dB fractional bandwidth, FBW = 21%), low insertion loss of 0.86 dB, and deep transmission zeros of −37.8 and −65 dB at 4.51 GHz and 6.89 GHz are presented. Two transmission zeros (4.07 GHz and 4.51 GHz) are placed between the two pass-bands and resulted in a −22 dB isolation. The compact size is $8.7 \times 8.7\,\text{mm}^2$ and the size reduction is 78.1%. It can be applied to the WLAN 802.11a/b/g systems.

## REFERENCES

1. Wolff, I., "Microstrip bandpass filter using degenerate modes of a microstrip ring resonator," *Electron. Lett.*, Vol. 8, No. 12, 302–303, Jun. 1972.
2. Zhu, L., P. M. Wecowski, and K. Wu, "New planar dual-mode filter using cross-slotted patch resonator for simultaneous size and loss reduction," *IEEE Trans. Microwave Theory & Tech.*, Vol. 47, No. 5, 650–654, May 1990.
3. Zhu, L., B. C. Tan, and S. J. Quek, "Miniaturized dual-mode bandpass filter using inductively loaded cross-slotted patch resonator," *IEEE Microw. Wireless Compon. Lett.*, Vol. 15, No. 1, 22–24, Jan. 2005.
4. Tu, W. H. and K. Chang, "Miniaturized dual-mode bandpass filter with harmonic control," *IEEE Microw. Wireless Compon. Lett.*, Vol. 12, No. 15, 838–840, Dec. 2005.
5. Wu, S., M. H. Weng, S. B. Jhong, and M. S. Lee, "A novel crossed slotted patch dual-mode bandpass filter with two transmission zeros," *Microwave Opt. Tech. Letters*, Vol. 50, No. 3, 741–744, Mar. 2008.
6. Hung, C. Y., M. H. Weng, S. B. Jhong, S. Wu, and M. S. Lee, "Design of the wideband dual mode bandpass filter using stepped impedance resonators," *Microwave Opt. Tech. Letters*, Vol. 50, No. 4, 1104–1107, Apr. 2008.
7. Su, Y. K., J. R. Chen, M. H. Weng, and C. Y. Hung, "Design of a miniature and harmonic control patch dual mode bandpass filter with transmission zeros," *Microwave Opt. Tech. Letters*, Vol. 50, No. 8, 2161–2163, Aug. 2008.
8. Weng, M. H., D. S. Lee, R. Y. Yang, W. Wu, and C. L. Liu, "A sierpinski fractal-based dual mode bandpass filter," *Microwave Opt. Tech. Letters*, Vol. 50, No. 9, 2287–2289, Sep. 2008.

9. Weng, M. H., L. S. Jang, and W. Y. Chen, "A Sierpinski-based resonator applied for low loss and miniaturized bandpass filters," *Microwave Opt. Tech. Letters*, Vol. 51, No. 2, 411–413, Feb. 2009.
10. Ye, C. S., Y. K. Su, M. H. Weng, and H. W. Wu, "Resonant properties of the sierpinski-based fractal resonator and Its application on low-loss miniaturized dual mode bandpass filter," *Microwave Opt. Tech. Letters*, Vol. 51, No. 5, 1358–1361, May 2009.
11. Chen, W. L. and G. M. Wang, "Effective design of novel compact fractal-shaped microstrip coupled-line bandpass filters for suppression of the second harmonic," *IEEE Microw. Wireless Compon. Lett.*, Vol. 19, No. 2, 74–76, Feb. 2009.
12. Xu, H. X., G. M. Wang, and C. X. Zhang, "Fractal-shaped UWB bandpass filter based on composite right/left handed transmission line," *Electron. Lett.*, Vol. 46, No. 4, 285–287, Feb. 2010.
13. Hanna, E., P. Jarry, E. Kerherve, and J. M. Pham, "A novel compact dual-mode bandpass filter using fractal shaped resonators," *IEEE International Conference on Electronics Circuits and Systems*, 343–346, 2006.
14. Sung, Y., "Dual-mode dual-band filter with band notch structures," *IEEE Microw. Wireless Compon. Lett.*, Vol. 20, No. 2, 73–75, Feb. 2010.
15. Sheta, A. F., N. Dib, and A. Mohra, "Investigation of new nondegenerate dual-mode microstrip patch filter," *IEE Proc. Microw. Antennas Propag.*, Vol. 153, No. 1, 89–95, Feb. 2006.
16. Liu, J. C., S. H. Chiu, C. P. Kuei, and B. H. Zeng, "A novel Minkowski-island-based fractal patch for dual-mode and miniaturization bandpass filters," *Microwave Opt. Tech. Letters*, Vol. 53, No. 3, 594–597, Mar. 2011.
17. Tsai, L. C. and C. W. Huse, "Dual-band bandpass filters using equal length coupled-serial-shunted lines and Z-transform techniques," *IEEE Trans. Microw. Theory Tech.*, Vol. 52, No. 4, 1111–1117, Apr. 2004.
18. Kuo, J. T., T. H. Yeh, and C. C. Yeh, "Design of microstrip bandpass filters with a dual-passband response," *IEEE Trans. Microw. Theory Tech.*, Vol. 53, No. 4, 1331–1337, Apr. 2005.
19. Huang, T. H., H. J. Chen, C. S. Chang, L. S. Chen, Y. H. Wang, and M. P. Houng, "A novel compact ring dual-mode filter with adjustable second-passband for dual-band applications," *IEEE Microw. Wireless Compon. Lett.*, Vol. 16, No. 6, 360–362, Jun. 2006.

20. Chen, J. X., T. Y. Yum, J. L. Li, and Q. Xue, "Dual-mode dual-band bandpass filter using stacked-loop structure," *IEEE Microw. Wireless Compon. Lett.*, Vol. 16, No. 9, 502–504, Sep. 2006.
21. Zhang, X. Y. and Q. Xue, "Novel dual-mode dual-band filters using coplanar-waveguide-fed ring resonators," *IEEE Trans. Microwave Theory & Tech.*, Vol. 55, No. 10, 2183–2190, Oct. 2007.
22. Wu, B., C. Liang, P. Qin, and Q. Li, "Compact dual-band filter using defected stepped impedance resonator," *IEEE Microw. Wireless Compon. Lett.*, Vol. 18, No. 10, 674–676, Oct. 2008.
23. Luo, S. and L. Zhu, "A novel dual-mode dual-band bandpass filter based on a single ring resonator," *IEEE Microw. Wireless Compon. Lett.*, Vol. 19, No. 8, 497–499, Aug. 2009.
24. Chiou, Y. C., C. Y. Wu, and J. T. Kuo, "New miniaturized dual-mode dual-band ring resonator bandpass filter with microwave C-sections," *IEEE Microw. Wireless Compon. Lett.*, Vol. 20, No. 2, 67–69, Feb. 2010.
25. Baik, J. W., L. Zhu, and Y. S. Kim, "Dual-mode dual-band bandpass filter using balun structure for single substrate configuration," *IEEE Microw. Wireless Compon. Lett.*, Vol. 20, No. 11, 613–615, Nov. 2010.
26. Cohen, N., "Fractal element antennas," *J. of Electron. Defense*, 48–49, 1997.
27. Zeland Software Inc., IE3D version 10.0, Jan. 2005.